

A method to model realistic particle shape and inertia in DEM

Jean-Francois Ferrellec · Glenn R. McDowell

Received: 14 December 2009 / Published online: 7 September 2010
© Springer-Verlag 2010

Abstract A simple and fast original method to create irregular particle shapes for the discrete element method using overlapping spheres is described. The effects of its parameters on the resolution of the particle shape are discussed. Overlapping spheres induce a non-uniform density inside the particle leading to incorrect moments of inertia and therefore rotational behaviour. A simple method to reduce the error in the principal moments of inertia which acts on the individual densities of the spheres is also described. The pertinence of the density correction is illustrated by the case of free falling ballast particles forming a heap on a flat surface. In addition to improve behaviour, the correction reduces also computational time. The model is then used to analyse the interaction between ballast and geogrid by simulating pull-out tests. The pulling force results show that the model apprehends better the ballast geogrid interlocking than models with simple representation of the shape of the particles. It points out the importance of modelling accurately the shape of particles in discrete element simulations.

Keywords Discrete element modelling · Shape · Inertia · Dynamics · Ballast · Geogrid

Abbreviation

DEM Discrete element method

1 Introduction

The discrete element method or DEM considers a granular material as consisting of particles interacting with each other and with walls through a contact law and Newton's 2nd law via an explicit time-stepping scheme [1]. The first DEM models, two-dimensional, used disks to represent the particles and were very basic. The introduction of clusters of disks to take into account irregular particle shapes led to some improvement [2]. However because of their two dimensions, these models could not represent real materials. By including rolling resistance at contact between simple disks, other DEM models indirectly reproduced the behavior of irregular particles [3–6]. These models reproduced the behavior of particles which surface is uniformly irregular as the rolling resistance acts isotropically around the disks. Hence they cannot reproduce the behavior of elongated particles. Most three-dimensional DEM models also use spheres to represent the particles as it makes the contact detection and force calculation easier than any other shape. Subsequently they can reproduce only qualitatively the behavior of granular materials and offer rather poor insight when it comes to quantitative measures. This restriction limits considerably the field of application of the method. Superquadrics were first used to remedy this restriction. The ellipsoid thus generated [7–10] led to some progress. The cylindrical shape has also been modeled [11]. But the need for a more quantitatively reliable model still remained as most of the natural shapes of granular material particles are irregular and angular. Models with polyhedrons [12–14] have been used to represent complex shapes but were quite demanding in terms of calculation. The concept of an agglomerate where spheres are bonded together to create complex shapes and simultaneously keep the contact detection and force calculation easy emerged [15, 16]. The number

J.-F. Ferrellec · G. R. McDowell (✉)
Nottingham Centre for Geomechanics,
Department of Civil Engineering,
University of Nottingham, University Park,
Nottingham NG7 2RD, UK
e-mail: glenn.mcdowell@nottingham.ac.uk

of balls required for realistic particle shapes made this approach computationally time-consuming. Wang et al. [17] proposed a similar clustering method where the volume of an irregular particle is filled with a regular arrangement of spheres but optimized afterwards by replacing groups of adjacent spheres by a bigger one to reduce the total number of spheres and therefore the calculation time. The model manages to render quite well the shape of irregular particles depending on the size of the small spheres at the beginning of the process but has the disadvantage of leading to rough or bumpy particle surfaces not representative of the real surface. Different approaches use overlapping spheres called clumps in which internal contacts are ignored and which behave as a rigid body [18]. Following this approach, Matsushima et al. [19] proposed a sophisticated dynamic process to fill the volume of a real particle with overlapping spheres in order to model sand grains. The first step consists of randomly creating spheres of different diameters inside the irregular volume. In the second step, the spheres are moved, expanded or shrunk using virtual forces to make them fit optimally within the boundaries. The virtual force acting on a sphere depends on its distance to the boundaries, weighted by spring constants for the motion or the expansion. However the initial random positions of the spheres and the adjustment of the virtual force parameters have a strong influence on the convergence of this optimization. The optimal conditions to produce satisfactory results have not yet been clearly established. Price et al. [20] also fitted spheres in the volume of real particles in an optimal way. Knowing one unique sphere can fit through four random points in space, they first filled the volume of the particle by repeatedly creating a sphere through four random points chosen on the surface of the particle. Afterwards they optimized this rough estimate by expanding or shrinking the spheres by minimizing locally the distance between the spheres and the surface of the particle. The optimization process proved more efficient to the authors of the present study when the four random points of the first step were chosen locally in the same area of the particle. Both the sphere generation and optimization make the method demanding in terms of calculation time and not easily applicable to samples containing dozens of different particle shapes.

Even if successful in reproducing irregular particle shapes, the methods described above all present disadvantages: the rough surface of the particle for the clustering method, unclear initial conditions for success of the dynamic method or too time-consuming calculations for the four points sphere fitting method. The drawback of overlapping spheres is the major problem of overlapping mass leading to a non-uniform density of the particle and hence an incorrect inertia tensor and centre of gravity, giving a false rolling resistance. The authors described a simple and fast technique to build irregular shapes with overlapping spheres

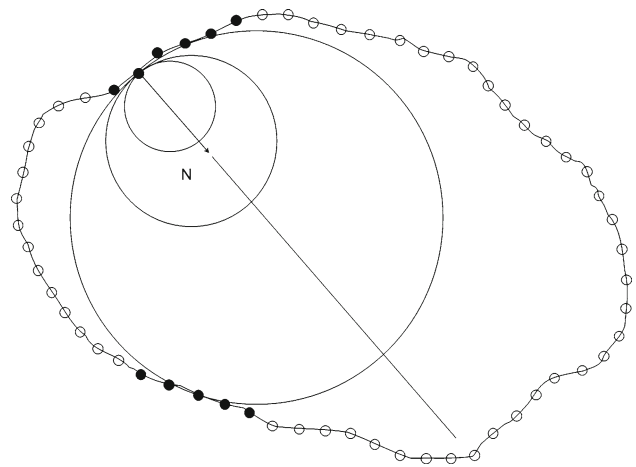


Fig. 1 Expansion of a sphere along the normal at a surface point inside the boundaries of the real particle

which offers the possibility of realistically rendering a real particle [21]. They pointed out the problem of incorrect mass distribution inside the particle, explained how to choose adequately differential densities for the spheres and reduce significantly the error in the particle inertia and finally applied it on an entire aggregate of railway ballast [22].

Geogrids are used in railway engineering to stabilize railway ballast and hence reduce its maintenance [23]. The geogrid, a rigid mesh, is laid horizontally inside the ballast. The interlocking between the geogrid and the ballast particles makes the ballast stiffer and hence less prone to irreversible deformations degrading the quality of the railway track. The authors built their realistic particle shape model to study the geogrid-ballast interaction.

This paper first briefly describes how to build an irregular shape of particle with overlapping spheres and how to adequately choose differential densities for the spheres to correct the inertia of the particle. Then it describes its application to understand the interaction between ballast and geogrid by using a standard pull-out test. This test is used to measure the efficiency of a geogrid and simply consists of pulling horizontally on a geogrid inserted in a box filled with ballast particles. The ability of the realistic DEM model to reproduce the test is discussed.

2 Particle shape

The method used here to reproduce the shape of a real particle with overlapping spheres requires the representation of the surface of this particle as a cloud of points in space. The particle shape resolution depends on the density of points on this surface: the higher the number of points, the better the resolution. Three dimensional scans based on stereophotogrammetry were used for this purpose. From two pictures of an object taken at two different angles, this method

Fig. 2 Effect of a decrease of d_{min} from top to bottom

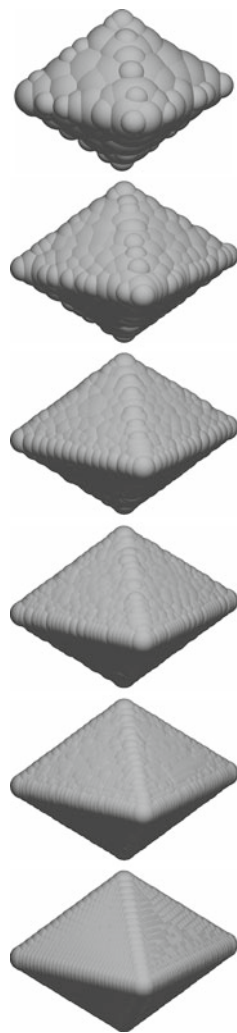


Table 1 Number of spheres used versus d_{min} when $r_{min} = 2$ mm and $p_{max} = 100$ %

d_{min} (mm)	0	0.1	0.2	0.3	0.5	1
Number of spheres used	2,312	952	546	332	188	87

allows to the numerical reconstitution of the surface of this object in space. If the object is scanned from different angles, then the complete surface of this object can be reconstituted numerically and represented by a mesh or cloud of nodes. For the purpose of this study, 41 ballast particles of different sizes have been scanned and stored as a mesh containing clouds of nodes to be used for clump formation in DEM.

In the present method (Fig. 1), the volume of the real particle is filled optimally with spheres of different sizes: from a point chosen randomly on the surface, a sphere is grown along its internal normal direction to the maximum extent possible inside the boundary of the particle. In other words, the expansion of the sphere continues until it reaches

Fig. 3 Effect of a decrease of r_{min} from top to bottom

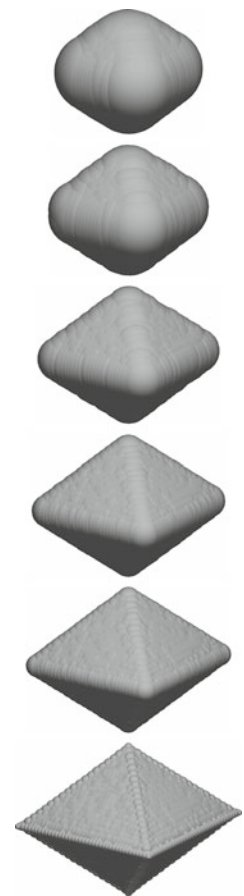


Table 2 Number of spheres used versus r_{min} when $d_{min} = 0.1$ mm and $p_{max} = 100$ %

r_{min} (mm)	0	2	4	5	7	9
Number of spheres used	1,439	952	702	485	264	125

another point on the surface of the particle. Then the process is repeated for other points on the surface of the particle. The number of spheres inside the clump is directly related to the number of points on the surface. If the density of points on the surface of the particle is high enough, then the process can theoretically lead to a clump composed of thousands of spheres. However such a clump would hardly be usable in a DEM simulation as it would require unreasonable calculation time. Different parameters have been included in the model to intentionally limit the number of spheres in the particles and hence reduce the computational time when they are used in DEM. As their characteristics have already been described in detail by Ferrellec and McDowell [21], they are only briefly outlined here.

If a surface node is already close to a previously created sphere (the solid black nodes in Fig. 1), then it might not be necessary to create another sphere at this node. When close to an existing one, the contribution of a sphere to the shape

Fig. 4 Effect of an increase of p_{max} from top to bottom

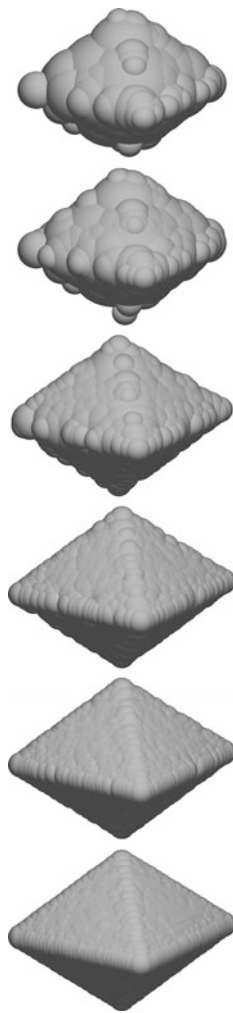


Fig. 5 Real ballast particle (top) and models with decreasing number of spheres from top to bottom

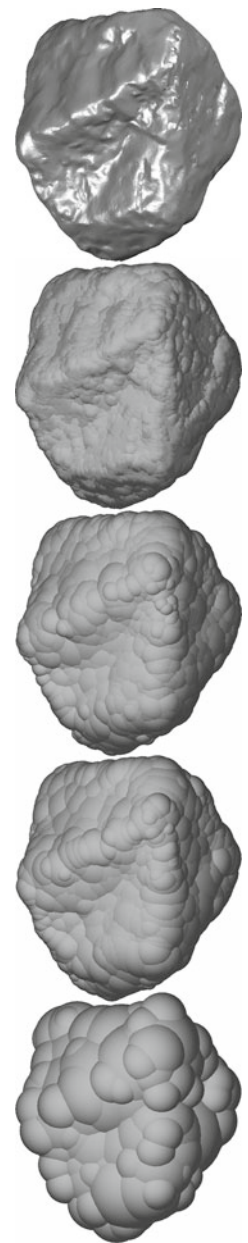


Table 3 Number of spheres used versus p_{max} when $d_{min} = 0.1$ mm and $r_{min} = 2$ mm

p_{max} (%)	3	5	10	20	30	100
Number of spheres used	73	123	239	460	668	952

would indeed be negligible. The proximity of a node to a neighbouring sphere is measured by the distance between the node and the surface of the sphere, precisely the distance between the node and the centre of the sphere minus its radius. If this distance is lower than a predetermined threshold d_{min} then no sphere is created at this node. The parameter d_{min} affects the uniformity of surfaces [21]. Figure 2 shows its influence on an octahedral shape using different values (Table 1). The smaller d_{min} is, the more even the surface. If the surface of the real particle is rough or presents irregularities, the spheres cannot expand inside the volume as they reach neighbouring nodes and hence remain small compared to the global size of the particle. These very small parasitic spheres spoil what should be a flat surface by actually

introducing an artificial roughness. It is possible to prevent this inconvenience by eliminating the spheres that have a radius smaller than a predetermined threshold r_{min} , limiting the spheres to the ones contributing effectively to the particle shape. The parameter r_{min} affects the sharpness of the particle [21] as seen on the octahedron in Fig. 3 using different values summarised in Table 2. The smaller r_{min} is, the sharper the edges. If the total number of spheres inside the particle is high even after tuning the parameters d_{min} and r_{min} , then it is possible to reduce it by simply fixing a maximum percentage p_{max} of selected nodes. If the number of nodes used reaches this maximum, then the spheres creation process is stopped. The parameter p_{max} has a global impact on the resolution of the particle as illustrated for an octahedron in Fig. 4 for

Table 4 Parameters sets for different numbers of spheres

Number of spheres	d_{min} (mm)	r_{min} (mm)	p_{max} (%)
5,500	0.1	2	10
800	0.1	0.5	1
400	1.14	1	1
100	1.8	3	1

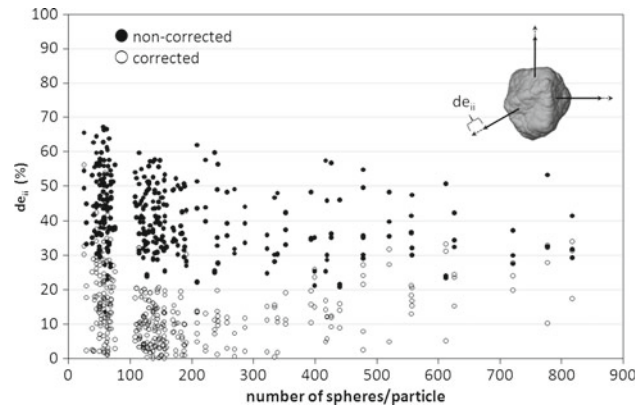


Fig. 6 Error in inertia principal moments (inertia tensor eigenvalues)

different values summarised in Table 3. The higher p_{max} is, the higher the resolution. Figure 5 shows the case of a real ballast particle using combinations of parameters specified in Table 4. A comparison of the effect of the different parameters of the model has shown that an acceptable representation of shape can be obtained using reasonably low values for r_{min} and p_{max} and high values for d_{min} .

3 Particle inertia

Building realistic particle shapes using overlapping spheres of the same density leads to an incorrect mass distribution inside the particle even if the overall mass of the particle is scaled to the real particle mass. Indeed because of larger overlapping in the middle of the particle, the particle density decreases from the middle to the surface of the particle as the spheres are all given the same density [22]. This concentration of mass in the middle leads only to an approximate centre of gravity and most importantly wrong eigenvalues of the inertia tensor. In problems where the dynamics of the particle is important, the resolution of this issue is fundamental as it may lead some particles to roll in an inappropriate way.

The authors proposed a method which consists in choosing adequately differential densities for the spheres. They showed that the inertia is greatly improved by setting the density of each sphere inversely proportional to its volume, leaving all spheres with the same mass instead of the same

Table 5 Size distribution of the ballast particles

Diameter range (mm)	(%)
0–22	1
22–32	18
32–40	44
40–50	32
50–63	5

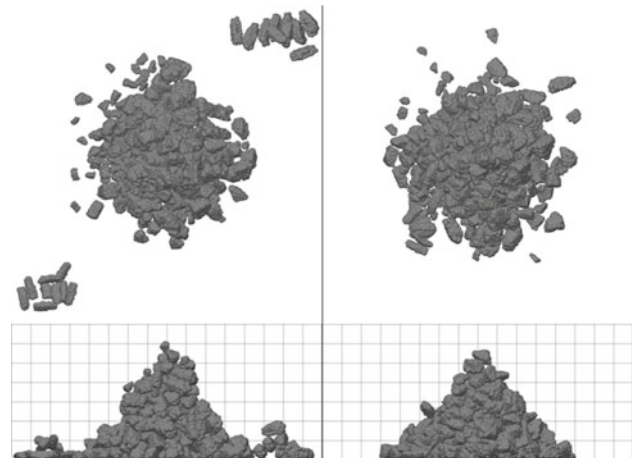


Fig. 7 Plan and side view of heaps for non-corrected (left) and corrected (right) particles

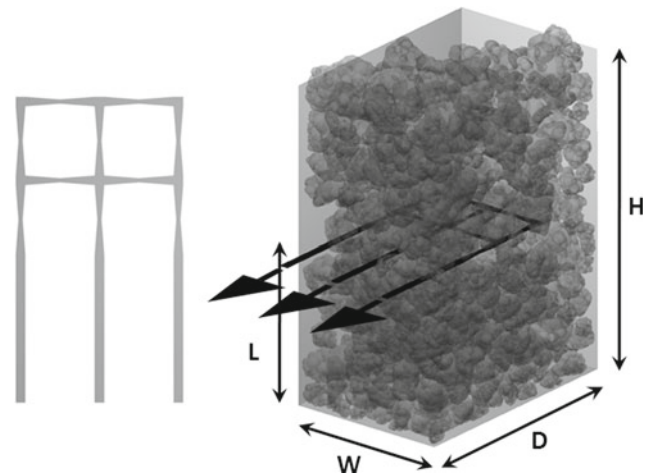
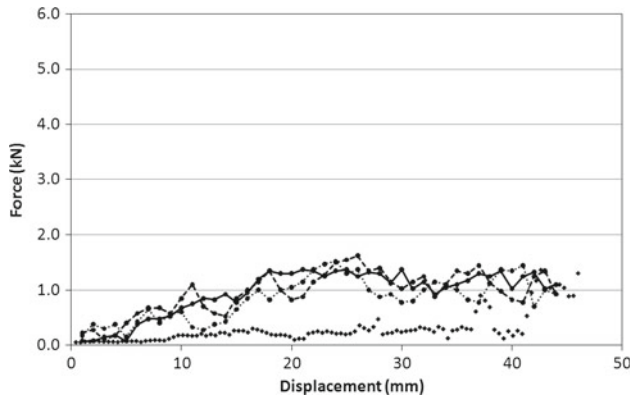
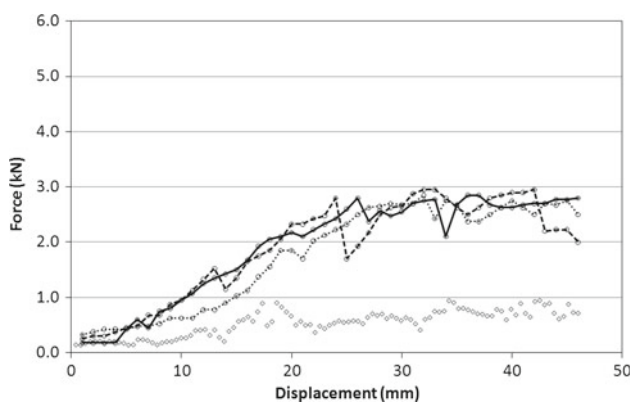


Fig. 8 Geogrid (left) and pull-out test configuration (right) with units in mm

density. The total mass of the particle is still scaled to be the same as that of the real particle but with a more uniform mass distribution inside the particle. Figure 6 shows the errors de_{ii} on the eigenvalues of the inertia tensor for a batch of 41 real ballast particles of different sizes (size distribution in Table 5) with and without the density correction and expressed as a percentage of the real eigenvalues using different numbers of spheres inside the particle. The error is clearly and signif-

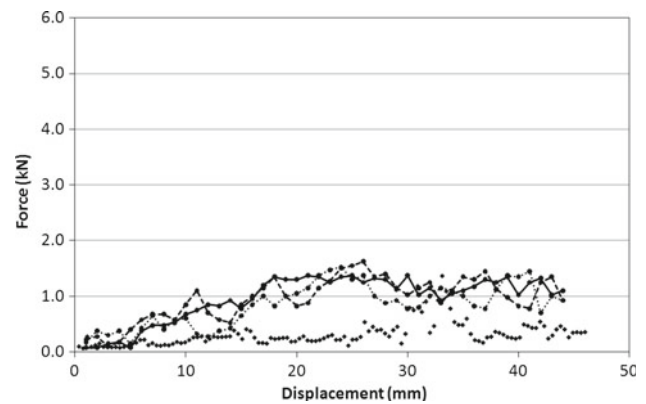
Table 6 Mechanical parameters of the simulation

Parameter	Spheres	Box	Geogrid
Friction coefficient	0.6	0	0.7
Stiffness (N/m)	6×10^7	6×10^7	9.76×10^8

**Fig. 9** Pulling force versus horizontal displacement with non-flattened surface below geogrid and no load on surface**Fig. 10** Pulling force versus horizontal displacement with non-flattened surface below geogrid and 500N load on surface

ificantly reduced when all spheres have the same mass. Figure 6 shows for example that the average error drops from approximately 45% to around 10% when the number of spheres per particle is between 100 and 200. The effect of the density correction on the directions of the principal axes of the inertia tensor is not significant. For example the error for particles containing around 300 spheres is less than 10% with or without correction. The density correction acts essentially on the magnitude of the principal moments of inertia.

The benefit of the correction might be questionable even if it significantly improves the inertia of the particle. The authors therefore performed a simple test involving the angle

**Fig. 11** Pulling force versus horizontal displacement with flattened surface below geogrid and no load on surface

of repose of an aggregate, an essential characteristic parameter of any granular material, in order to assess the pertinence of the correction. The test simply consists in letting ballast particles fall freely from 1m above a flat surface to form a heap. Each test simulation involves 10 batches of 41 different ballast particles of different sizes giving a total of 410 particles or 22530 spheres, with an average of 55 spheres per particle. The particle size distribution is summarised in Table 5. A series of simulations using different sets of mechanical parameters for the particles were performed [22]. The most interesting results were obtained for a contact stiffness of 10^7 N/m, a friction coefficient of 0.7 for the sphere and 0.5 for the flat surface. Figure 7 shows the final heap obtained with and without density correction, or in other words with (almost) correct and with incorrect inertia. This case shows the importance of inertia correction. Each particle of a given shape is generated at the same point. This point however varies slightly for each shape and can be eccentric but the sequence and initial points of the generated particles are identical for both simulations. Then any difference in behaviour between the two simulations arises only from the different inertias as all the other conditions are strictly identical. The elongated particles obviously pile up away from the heap in the non-corrected case. The incorrect inertia of these particles makes them roll away more easily than they should as confirmed by the corrected case where they are part of the heap. This particular test shows that inertia correction is important at least in cases involving a dynamic process like granular material handling. In addition to improve the mass distribution inside the particle, the correction improves significantly the calculation speed in DEM simulation. The calculation time step in DEM increases when the mass of the spheres increases, making the simulation faster. A non-corrected particle will indeed contain spheres with smaller masses than its corrected counterpart and then will require more calculation time. As an illustration, the non-corrected case simulation of Fig. 7 took 303h to run, when the corrected one took only 113h.

4 Application to geogrid-reinforced railway ballast

Geogrids are laid inside ballasts to stabilise railway tracks. Their efficiency can be measured using a pull-out test which consists in horizontally pulling a geogrid embedded in ballast particles confined in a box (Fig. 8). The force necessary to pull the geogrid is measured and used to assess the quality of the geogrid: the higher the force, the better the geogrid. This test has been simulated using the realistic particle shapes DEM model. The box was filled by randomly creating the ballast particles in a hopper above the box and letting them fall under gravity. The bottom half of the box was first filled. Then the geogrid modelled by walls was inserted using two options: either by flattening the surface with a horizontal wall and then creating the geogrid above the surface, or by deleting obstructing particles near the surface and then creating the geogrid between the remaining ones. Then using the hopper again, the top half of the box was filled to the top surface. Both options give an approximate total mass of around 36kg of ballast in the box giving an apparent density of $1,500\text{ kg/m}^3$. The mass of ballast above the geogrid is 16.9kg for the non-flattened case and 18.2 kg for the flattened, explained by the fact that more free space is available in the geogrid apertures. An additional load can be added on the top of the ballast using heavy spheres larger than the ballast particles. After the filling process and eventual stabilisation of the particles under loading, the geogrid was moved horizontally at 10 mm/s. The particle size distribution is summarised in Table 5. The parameters characterising the ballast particles, the box and the geogrid have been imported from a previous study on geogrid-ballast interaction and are summarised in Table 6.

Figure 9 shows a comparison of the pulling force between three experimental tests and the simulation when the surface below the geogrid is not flattened and without any load on the surface of the particles. The circle markers interconnected with lines indicate experimental results while the loz-

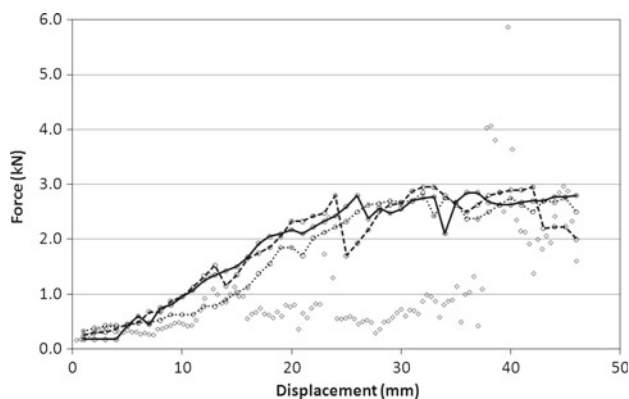


Fig. 12 Pulling force versus horizontal displacement with flattened surface below geogrid and 500N load on surface

enge markers indicate simulation results. The experimental results show a continuous and significant increase of the pulling force followed by a stabilisation after 20 mm of displacement around 1kN. The simulation on the other hand increases very slowly until 35 mm, shows higher fluctuation and finally reaches a level of pulling force similar to the experimental one. This can be explained by the fact that the geogrid in simulation is completely rigid while in experimental conditions it is actually flexible. The deformability of the geogrid in experiments allows a more progressive increase of the pulling force. Figure 10 shows a similar comparison for a 500N load on the top surface of the particles. The experimental results show again a continuous increase of the force followed by a stabilisation at a higher level around 2.5kN. The simulation force however, even if increasing at a higher level than without load, remains at a level much lower than the experimental one. Figure 11 shows a comparison of the same three experimental tests with the simulation where the surface below the geogrid is flattened. The pulling force of the simulation presents more fluctuations, probably due to more particles interlocked with the geogrid and being pushed by the geogrid. As the surface has been flattened, more space became available for the particles above the geogrid creating more interlocking. This is confirmed on Fig. 12 where the load on the top surface is 500N and where the fluctuations are more frequent and higher in magnitude reaching a level comparable to the experimental one. The non-deformability of the geogrid in the simulation is also probably partially responsible for the fast fluctuations of the force. Figure 13 shows a sequence of forces between particles corresponding to the fluctuation of pulling force observed in Fig. 12 for a displacement of about 23 mm. Each contact force between two spheres of the particles is represented by a black cylinder whose radius depends on the intensity of the force. The sequence clearly shows a high contact force on the geogrid which is transmitted through particle-particle contacts until it reaches the front wall of the box from where the geogrid is pulled. Then later this force chain is broken and the pulling force drops. The fluctuations of the pulling forces are clearly connected to the formation/destruction of arches inside the ballast pulled by the geogrid. Previous studies using simple agglomerates to represent angular particles in DEM simulations show much less fluctuation [24]. The much larger fluctuations observed here and in the experimental tests, seem to indicate that better interlocking is achieved with the present model.

Globally, the results show the importance of the initial conditions of the test including the filling of the box and the insertion of the geogrid. The interlocking between the geogrid and the ballast is strongly dependent on the filling process and compaction of the ballast. A particular attention to these conditions is necessary to be able to reproduce correctly the pull-out test results. The geogrid model requires

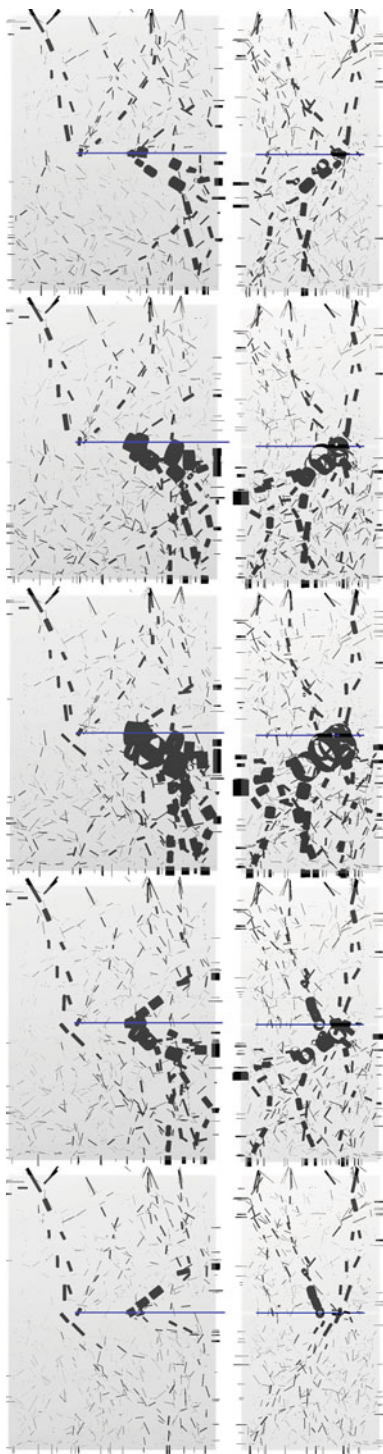


Fig. 13 Sequence of contact force network: side (*left*) and front (*right*) views

further investigation to assess the impact of the deformability of the geogrid on the results. A simple geogrid made of bonded spheres which could transmit tensile forces and moments would probably be appropriate.

5 Conclusion

A fast and simple original method to create complex irregular particle shapes for DEM using overlapping spheres has been developed. The method includes only three parameters that act on the accuracy of the shape reproduction and the number of spheres per particle. Real particles can be modelled precisely in terms of shape using a reasonable number of spheres. Overlapping spheres generate a non-uniform distribution of mass inside the particle leading to incorrect moments of inertia and hence affecting the rotation of the particle in simulation. Giving the same mass to all spheres inside the particle and still keeping a global mass equal to that of the real particle improves the mass distribution and significantly reduces the error in inertia. In addition, the density correction reduces calculation time because small spheres no longer have small masses. A full representative range of ballast particles of different sizes has been built using this method. The mass distribution correction seems to have a non-negligible impact in processes involving dynamics like the formation of a heap. The behaviour of geogrid-reinforced ballast aggregate has been analysed through DEM simulations of pull-out tests. The monitored pulling force shows fluctuations related to a succession of particle arching formation and destruction. The ability of the model to reproduce the fluctuations shows that the model has achieved the reproduction of the interlocking between the geogrid and the particles. It points out the importance of modelling accurately the shape of the particles in DEM.

Further investigation will focus on the impact of the resolution of the particles on the results of the pull-out tests and evaluate the optimal number of spheres per particle necessary. Preliminary work will first be performed on the geogrid model to take into account its flexibility. The model associated with the pull-out test will be used in the end to optimise the geogrid.

Acknowledgments The authors would like to thank EPSRC for their financial support for this project and Tensar International for their technical support.

References

1. Cundall, P.A., Strack, O.D.L.: A discrete numerical model for granular assemblies. *Géotechnique* **29**(1), 47–65 (1979)
2. Thomas, P.A., Bray, J.D.: Capturing nonspherical shape of granular media with disk clusters. *J. Geotech. Geoenviron. Eng.* **125**, 169–178 (1999)
3. Iwashita, K., Oda, M.: Rolling resistance at contacts in simulation of shear band development by DEM. *J. Eng. Mech.* **124**, 285–292 (1998)
4. Iwashita, K., Oda, M.: Micro-deformation mechanism of shear band process based on modified distinct element method. *Powder Technol.* **109**, 192–205 (2000)

5. Jiang, M.J., Yu, H.-S., Harris, D.: A novel discrete model for granular material incorporating rolling resistance. *Comput. Geotech.* **32**(5), 340–357 (2005)
6. Jiang, M.J., Leroueil, S., Zhu, H.-H., Yu, H.-S., Konrad, J.M.: Two-dimensional discrete element theory for rough particles. *Int. J. Geomech.* **9**(1), 20–33 (2009)
7. Williams, J.R., Pentland, A.P.: Superquadric and modal dynamics for discrete elements in interactive design. *Eng. Comput.* **9**, 115–127 (1992)
8. Lin, X., Ng, T.T.: A three-dimensional discrete element model using arrays of ellipsoids. *Géotechnique* **47**(2), 319–329 (1997)
9. Mustoe, G.G.W., Miyata, M.: Material flow analyses of noncircular-shaped granular media using discrete element methods. *J. Eng. Mech.* **127**(10), 1017–1026 (2001)
10. Cleary, P.W.: Large scale industrial DEM modelling. *Eng. Comput.* **21**, 169–204 (2004)
11. Pournin, L., Weber, M., Tsukahara, M., Ferrez, J.-A., Ramaioli, M., Liebling, Th.M.: Three-dimensional distinct element simulation of spherocylinder crystallization. *Granul. Matter* **7**(2-3), 119–126 (2005)
12. Hart, R., Cundall, P.A., Lemos, J.: Formulation of a three-dimensional distinct element model – Part II. Mechanical calculations for motion and interaction of a system composed of many polyhedral blocks. *Int. J. Rock Mech. Min. Sci. Geomech. Abstr.* **25**(3), 117–125 (1988)
13. Abou-Chakra, H., Baxter, J., Tüzün, U.: Three-dimensional particle shape descriptors for computer simulation of non-spherical particulate assemblies. *Adv. Powder Technol.* **15**(1), 63–77 (2004)
14. Lee, Y., Fang, C., Tsou, Y.-R., Lu, L.-S., Yang, C.-T.: A packing algorithm for three-dimensional convex particles. *Granul. Matter* **11**(5), 307–315 (2009)
15. McDowell, G.R., Harireche, O.: Discrete element modelling of yielding and normal compression of sand. *Géotechnique* **52**(4), 299–304 (2002)
16. Thornton, C., Liu, L.: How do particles break?. *Powder Technol.* **143**(144), 110–116 (2004)
17. Wang, L., Park, J., Fu, Y.: Representation of real particles for DEM simulation using X-ray tomography. *Construct. Build. Mater.* **21**, 338–346 (2007)
18. Lu, M., McDowell, G.R.: The importance of modelling ballast particle shape in DEM. *Granul. Matter* **9**(1–2), 71–82 (2007)
19. Matsushima, T., Saomoto, H., Matsumoto, M., Toda, K., Yamada, Y.: Discrete element simulation of an assembly of irregularly-shaped grains: quantitative comparison with experiments. In: 16th ASCE Engineering Mechanics Conference, July 16–18, 2003 University of Washington, Seattle (2003)
20. Price, M., Murariu, V., Morrison, G.: Sphere clump generation and trajectory comparison for real particles. In: *Discrete Element Methods 2007 Conference*, 27–29 August 2007, Brisbane, Australia (2007)
21. Ferrellec, J.-F., McDowell, G.R.: A simple method to create complex particle shapes for DEM. *Geomech. Geoeng.* **3**(3), 211–216 (2008)
22. Ferrellec, J.-F., McDowell, G.R.: Modelling realistic shape and particle inertia in DEM. *Géotechnique* **60**(3), 227–232 (2010)
23. Selig, E.T., Walters, J.M.: *Track Geotechnology and Substructure Management*. Thomas Telford, London (1993)
24. McDowell, G.R., Harireche, O., Konietzky, H., Brown, S.F., Thom, N.H.: Discrete element modelling of geogrid-reinforced aggregates. In: *Proceedings ICE—Geotechnical Engineering*, 159 (GE1), pp. 35–48 (2006)